

## **X-RAY FLUORESCENCE MICROTOMOGRAPHY ANALYZING PROSTATE TISSUES.**

**Gabriela R. Pereira<sup>1</sup>, Henrique S. Rocha<sup>1</sup>, Cristiane Calza<sup>1</sup>, Marcelino J. Anjos<sup>2</sup>, Carlos A. Pérez<sup>3</sup> and Ricardo T. Lopes<sup>1</sup>**

<sup>1</sup> Nuclear Instrumentation Laboratory - COPPE/UFRJ  
P.O. Box 68509  
21941-972, Rio de Janeiro, RJ, Brazil  
[gabriela@lin.ufrj.br](mailto:gabriela@lin.ufrj.br)  
[henrique@lin.ufrj.br](mailto:henrique@lin.ufrj.br)  
[ccalza@lin.ufrj.br](mailto:ccalza@lin.ufrj.br)  
[ricardo@lin.ufrj.br](mailto:ricardo@lin.ufrj.br)

<sup>2</sup> Physics Institute – UERJ  
20559-900 Rio de Janeiro, RJ, Brazil  
[marcelin@lin.ufrj.br](mailto:marcelin@lin.ufrj.br)

<sup>3</sup> Brazilian Synchrotron Light Laboratory - LNLS  
P.O. Box 6192  
13083-970 Campinas, SP, Brazil  
[perez@lnls.br](mailto:perez@lnls.br)

### **ABSTRACT**

The objectives of this work is to determine the elemental distribution map in reference samples and prostate tissue samples using X-Ray Fluorescence Microtomography (XRFCT) in order to verify concentrations of certain elements correlated with characteristics observed by the transmission microtomography. The experiments were performed at the X-Ray Fluorescence Facility of the Brazilian Synchrotron Light Laboratory. A quasi-monochromatic beam produced by a multilayer monochromator was used as an incident beam. The transmission CT images were reconstructed using filtered-back-projection algorithm, and the XRFCT images were reconstructed using filtered-back-projection algorithm with absorption corrections.

### **1. INTRODUCTION**

The human prostate is a gland, found only in men, whose function is essencial in male reproductive system. Benign Prostatic Hyperplasia (BPH) is the most common benign neoplasm. It is not a cancer but progressive enlargement of the prostate gland chokes the urethra making it difficult to empty the urinary bladder. BPH can be confused with prostate cancer because they share similar symptoms. It is therefore important to be able to distinguish one from the other [1].

In recent years, there has been growing interest in understanding the exact role played by trace elements in several diseases. The biological function of some metal ions in combination with an investigation of element distribution patterns in malignant and in normal human tissues of cancer patients can give some indication of the effect of metal ions on carcinogenesis [2,3,4]. The biochemistry of iron, copper and zinc, suggests that these metals

may play an important role in carcinogenesis and the fluorescence mapping of these metals can be very important to find evidence linking these metals to diseases.

The main advantage of X-ray Fluorescence Microtomography (XRFCT) is that it is a non-destructive technique. Following analysis using this technique, samples may be analyzed with others techniques, such as x-ray diffraction [5]. In addition, in contrast to micro XRF analysis, XRFCT does not require sample preparation, such as planar mode. Micro XRF requires that samples be embedded/fixed in paraffin, in order to achieve ultra fine accurate slices (of approximately 15 microns) [6]. XRFCT, on the other hand, does not require this sort of sample preparation; it is not necessary to cut the sample to analyze the tomographic plane.

In X-Ray Fluorescence (XRF) microtomography an X-ray beam is used for the excitation of the elements inside of the sample and the fluorescence from one or more elements is measured. At each projection angle the line integral of the fluorescence along the beam inside the sample is measured. A single tomographic slice is collected by translating and rotating the sample on a 2-D grid. The spatial resolution of this technique is limited only by the size of the focused X-ray beam, which can be less than 1 micrometer. Data acquisition of X-ray fluorescence microtomography results in bi-dimensional data image representations called sinograms. A sinogram consists of line scans taken at every rotational angle. For each emission line of the fluorescence spectrum there is a separate sinogram. In general, a sinogram plots the property measured by the setup over the direction perpendicular to the beam and the angle of rotation. The tomogram which is a two dimensional slice across the sample can be reconstructed from the sinogram applying the appropriate algorithm [7,8]. A significant requirement of the method is that the absorption of the fluorescence X-rays within the sample must be small. The elements that can be measured are therefore a strong function of the bulk composition and size of the sample.

In this work reference samples and prostate tissue samples have been analyzed to verify the concentration of some elements correlated with characteristics and pathology of each tissue observed by X-ray transmission microtomography (CT).

## 2. EXPERIMENTS

This work presents the development of a system to study X-ray fluorescence microtomography at the X-Ray Fluorescence Facility (D09B-XRF) at the Brazilian Synchrotron Light Laboratory (LNLS), Campinas, Brazil. A quasi-monochromatic beam produced by a multilayer monochromator at 12 keV,  $\Delta E/E = 0.03$  collimated to a  $200\mu\text{m} \times 200\mu\text{m}$  area with a set of slits, was used to sample excitation. The crystal monochromator consists of W-C and 75 layer pairs.

The intensity of the incident beam was monitored with an ionization chamber placed in front of it, before the sample. A schematic of the experimental setup for X-ray fluorescence microtomography using a multilayer monochromatic beam is shown in Figure 1.

The sample was placed on a high precision goniometer and translation stages, which respectively allow rotation as well as translation perpendicular to the beam. Fluorescence photons were collected with an energy dispersive HPGe detector (CANBERRA Industries

inc.) placed at  $90^\circ$  to the incident beam, while transmitted photons were detected with a fast NaI (Tl) scintillation counter (CYBERSTAR-Oxford anfyisik) placed behind the sample on the beam direction.

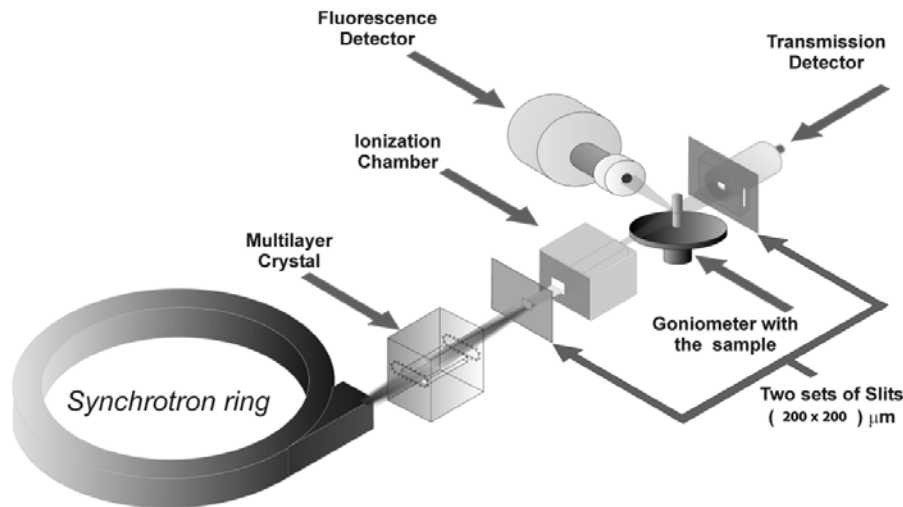


**Figure 1. The experimental arrangement for an X-ray fluorescence microtomography measurement.**

In one projection, samples were positioned in steps of  $200\mu\text{m}$  (actual beam size) perpendicular to the beam, covering the whole transversal section of the sample proof.

Each single value in a projection is obtained by measuring the fluorescence radiation emitted by all pixels along the beam. The object is then rotated, and another projection is measured. Projections were obtained in  $3^\circ$  steps, until the object had rotated a full  $180^\circ$ . The selected measuring time was 5s for each scanned point. The experiment takes about 3 hours for each sample.

A reference sample made of polyethylene filled with a standard solution of gallium was first analyzed and used as a test sample. Specifically, the sample was comprised of a polyethylene cylinder of 2.0 mm of diameter containing an internal cylinder of 1.0 mm of diameter, filled with a standard solution of gallium,  $200\mu\text{g/g}$  [5].

As a second part of the experiments, XRF microtomographies were performed on human prostate tissue samples with BPH. The component tissues were identified by the pathologist who made the sample available. The tissues were cut in cylindrical form with 1.5 mm to 2.0 mm thickness by 4.0 mm to 5.0 mm of height and were frozen and dried before being analyzed.

The X-ray transmission images were reconstructed using a filtered-back projection algorithm and the X-ray fluorescence tomography images were reconstructed using a filtered-back projection algorithm with absorption corrections. The filtered-back projection algorithm was

implemented in matlab and the absorption corrections matrix was calculated using mkkcorr, a part of the software ScatterTomo developed by Brunetti to calculate the correction factor of absorption [9].

### 3. RESULTS AND DISCUSSION

Results for the reference sample made of polyethylene are shown in Figure 2.

The images in Figure 2 show the X-ray transmission microtomography at 12 keV (Fig. 2a), the absorption corrections matrix (Fig. 2b) and the XRF microtomography of gallium without absorption corrections (Fig. 2c) and with absorptions corrections (Fig. 2d).

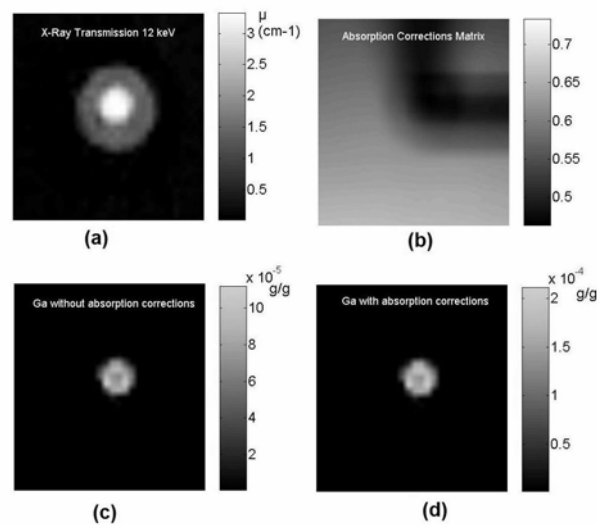


**Figure 2. X-ray transmission microtomography of a reference sample at 12 keV (a), absorption corrections matrix of the reference sample (b), XRF microtomography of Ga without absorption corrections (c) and XRF microtomography of Ga with absorption correction (d).**

It can be observed analyzing the images that while the X-ray transmission tomography shows the polyethylene matrix and the internal cylinder with gallium solution, the XRF tomographies show only those regions where the elements of interest were localized, in this case gallium. These tomographies show the viability of fluorescence microtomography and confirm that this technique can be used to complement others techniques for sample characterization.

Upon first sight, it is extremely difficult to attest the influence of absorption correction. However, upon analyzing the concentrations, it is possible to confirm that the influence is significant. It can be verified that there is a considerable difference in concentrations between

images reconstructed with absorption correction and those without absorption correction, even if the sample is small. X-ray fluorescence microtomography, reconstructed with absorption correction, shows a mean value of concentration of about 200 ppm. Whereas X-ray fluorescence microtomography, reconstructed without absorption correction, shows a mean value of about only 100 ppm, which is fifty percent less than the real value.

X-ray fluorescence microtomographies were performed on human prostate tissue samples. Three prostate samples with BPH for tree different patients were analyzed.

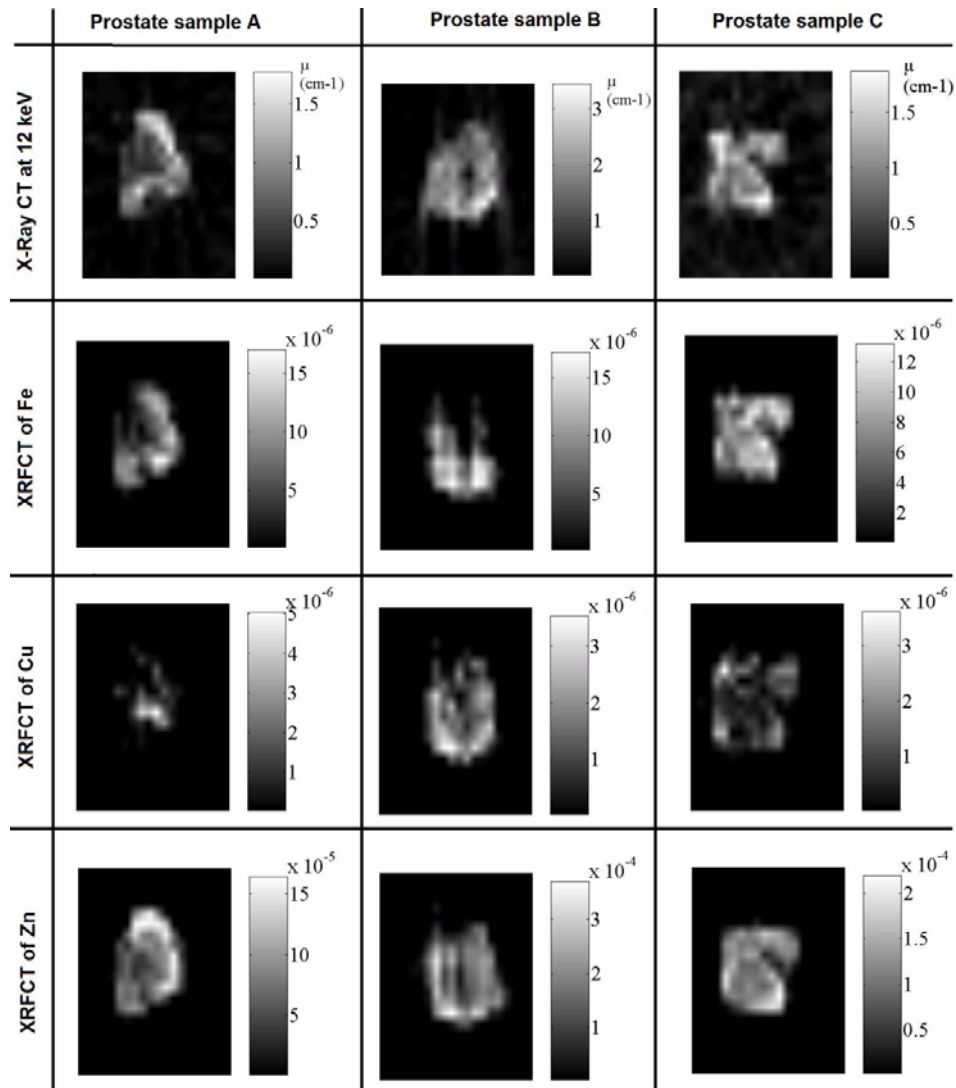


**Figure 3. X-ray transmission microtomographies (X-Ray CT) and XRF microtomographies (XRFCT) of iron, copper and zinc in human prostate BPH samples.**

The result for human prostate samples is shown in Figure 3. Each column in the Figure 3 shows the results for each prostate tissue sample separately. For each sample it was reconstructed the X-ray transmission microtomography image and the XRF microtomographies images of Fe, Cu and Zn.

Analyzing the XRF microtomographies of human prostate tissue sample fragments, it was possible to see the elemental distribution of iron, copper and zinc. It was verified that these tissues have a smaller concentration of copper and iron than zinc and the mean concentration of zinc in the BPH samples is about 150 to 300  $\mu\text{g/g}$ .

In the XRFCT image of iron in the prostate sample B, it can be seen that there is a flaw in the iron fluorescence distribution image. There is not iron in the entire sample. It is not known yet why in this sample the distribution of Fe is not homogeneous but this information can be important when comparing these results with healthy tissues.

Although trace elements Fe, Cu, and Zn are extremely common, assessment of their amounts is crucial for disease diagnostics. Both excess and deficiency of trace elements have been associated with many diseases including cancer. . It is necessary to measure more samples and quantify the difference in concentration in one sample and between normal and abnormal tissues to use the X-ray fluorescence microtomography as an analytic tool to analyze biological tissues. Pathologist-oncologist cooperation would be most advantageous for future research in this area.

The radial streak effects that can be visualized in tomographic reconstructions are because of the low counting statistic in each projection. The images were not processed.

### 3. CONCLUSIONS

The reference sample shows the viability of fluorescence microtomography and confirm that this technique can be used to complement others techniques for sample characterization. Analyzing these images, it is verified that it is very important to use the algorithm with absorption corrections to get the corrected value of concentration.

Analysis of the biological samples utilized led to the discovery of the elemental distribution of iron, copper and zinc and to the verification that these tissues have a smaller concentration of copper and iron than zinc.

It will be necessary to measure more samples and quantify the difference in concentration in one sample and between normal and abnormal tissues to use the X-ray fluorescence microtomography as an analytic tool to analyze biological tissues.

The better definition of the interfaces in X-ray fluorescence images was impressing and the spatial resolution of the system can be optimized as a function of the application. The experimental set up at XRF-LNLS has shown to be very promising and this effort at implementing X-ray fluorescence microtomography was justified by the high quality of the images obtained.

## ACKNOWLEDGMENTS

This Project received support and funding from the Conselho Nacional de Desenvolvimento Científico e Tecnológico (CNPq), Fundação de Amparo à Pesquisa do Estado do Rio de Janeiro (FAPERJ) and Laboratório Nacional de Luz Síncrotron (LNLS).

## REFERENCES

1. W.M. Kwiatek, A. Banás, K. Banás, G. Cinque, G. Dyduch, G. Falkenberg, A. Kisiel, A. Marcelli, M. Podgórczyk, "Micro and bulk analysis of prostate tissues classified as hyperplasia", *Spectrochimica Acta part B*, **62**, pp. 707-710 (2007).
2. T. Magalhães, A. von Bohlen, M.L. Carvalho, M. Becker, "Trace elements in human cancerous and healthy tissues from the same individual : A comparative study by TXRF and EDXRF", *Spectrochimica Acta part B*, **61**, pp.1185-1193 (2006).
3. G.J. Naga Raju, P. Sarita, M. Ravi Kumara, G.A.V. Ramana Murtya, B. Seetharami Reddy, S. Lakshminarayanaa, V. Vijayanb, P.V.B. Rama Lakshmic, Satyanarayana Gavarasanad, S. Bhuloka Reddy, "Trace elemental correlation study in malignant and normal breast tissue by PIXE technique", *Nucl. Instr. and Meth. B*, **247**, pp.361-367 (2006).
4. T. Wu , Sempos C T, Freudenheim J L, P. Muti, E. Smit., "Serum iron, copper, and zinc concentrations and risk of cancer mortality in US adults", *Annals of Epidemio*, **14-3**, pp.195-201 (2004).
5. G.R. Pereira, R.T. Lopes, M.J. Anjos, H.S. Rocha, C.A. Pérez, "X-ray Fluorescence Microtomography Analyzing Reference Samples", *Nucl. Instr. and Meth. A*, **579**, pp.322-325 (2007).
6. J. Chwiej, M. Szczerbowska-boruchowska, S. Wojcik, G. Falkenberg, Z. Stegowski, Z. Setkowicz, "Preparation of tissue samples for X-ray fluorescence microscopy", *Spectrochimica Acta part B*, **60**, pp.1531-1537 (2005).
7. R. Cesareo, S. Mascarenhas, "A new tomographic device based on the detection of fluorescent X-rays.", *Nuclear Instruments and Methods A*, **277**, pp.669-672 (1989).
8. J.P. Hogan, R. A. Gonsalves, A. S. Krieger, "Fluorescent computer tomography: a model for correction of X-ray absorption", *IEEE Trans. Nucl. Sci.*, **38**, pp.1721- 1727(1991).
9. A. Brunetti, B. Golosio, "Software for X-ray fluorescence and scattering tomographic reconstruction", *Comput. Phys. Commun.*, **141**, pp.412-425 (2001).